

GPO PRICE \$

CFSTI PRICE(S) \$

Hard copy (HC)

Microfiche (MF)

653 July 65

R-18
THE ABSOLUTE PHOTOMETRY OF THE ZODIACAL LIGHT

L. L. Smith, F. E. Roach* and R. W. Owen

Central Radio Propagation Laboratory
National Bureau of Standards, Boulder, Colorado

and

Hawaii Institute of Geophysics
University of Hawaii, Honolulu, Hawaii

UNCLASSIFIED 29493

Abstract—Interpretation is made of photometric records obtained at the Haleakala Observatory during six nights between August 1961 and June 1962. An interference filter centered on wavelength 5300 Å was used. After allowance for the airglow continuum and the integrated starlight, the residual is interpreted as due to zodiacal light. The brightness of the zodiacal light is tabulated for that part observable in the night sky. Graphical representations illustrate the distribution of brightness in ecliptic coordinates.

FEATHOR

I. INTRODUCTION

As a part of the airglow-zodiacal light program of the Haleakala Observatory of the Hawaii Institute of Geophysics (latitude N 20°.7, longitude W 156°.16), a photometer having an interference filter centered on wavelength 5300 Å was used in systematic observations of the night sky during the period from May 1961 to September 1962.

*The paper was prepared while FER was the recipient of a Senior Research Scholarship at the East-West Center of the University of Hawaii.

FACILITY FORM 602

(NASH CR OR TMX OR AD NUMBER)

(CATEGORY)

(PAGES)

(CODE)

(ACCESSION NUMBER)

(THRU)

N65-29493

The observing program involved scanning the sky in a series of almucantars at zenith distances 80° , 75° , 70° , 60° , 40° plus the zenith. In addition to the photometer (designated by us as RP), the alt-azimuth mount carried (a) a birefringent filter photometer for the study of the night airglow ⁽¹⁾ and (b) a polarimeter-photometer used by J. L. Weinberg ⁽²⁾ for a detailed study of the polarization (and photometry) of the zodiacal light. An auxiliary zenith photometer having a built-in and absolutely calibrated standard light was operated during all the observations ⁽³⁾ making it possible to obtain the calibration of the RP photometer by comparison of the simultaneous zenith sky readings throughout a night.

II. THE OBSERVATIONAL MATERIAL

The six nights included in the study (Table 1) were distributed throughout the year in approximately 2-month intervals. The principal reason for such a spread was to give a complete coverage of the astronomical sky for a photometric study of the integrated starlight especially in the Milky Way. ^{In}the present study, we have avoided galactic latitudes less than 30° in order to minimize uncertainties due to corrections for integrated starlight. Subsequently, we plan to return to the Milky Way study.

The large ensemble of data (more than one million individual readings) resulted in a library of print-outs of the absolute brightness of the night sky referred to outside the atmosphere for each degree of the sky and for the several almucantars involved in each sky survey.

The data have been examined in both systematic and specialized ways. An example of systematic use was the plotting of the 40° zenith distance readings for each half hour of sidereal time. An example of a specialized use of the data was the detailed coverage of the region near the ecliptic pole for which plots for each 5-minute survey were made over an extended period in order to delineate the details. We have been able to make corrections for errors in azimuth settings by comparison of peaks of maximum star deflections with their computed azimuths. Based on such comparisons, we believe that an individual azimuth is known to about $\pm 5^\circ$, not good enough for any finesse concerning the photometric axis of the zodiacal light but consistent with the 4° field of view of the photometer. Our final results based on a large quantity of data are probably good to $\pm 2^\circ$ in the various coordinates.

We have referred the readings to outside the atmosphere by allowing for (a) the extinction of the lower atmosphere plus ozone, (b) the scattering of the lower atmosphere and (c) the increase of

the airglow component toward the horizon. Some comment is in order on the problem of correcting for scattered light. We have used the tables by Ashburn⁽⁴⁾ who made numerical integrations of Rayleigh scattering for (a) a uniform sky with all the light coming from astronomical sources (assumed to be at an infinite distance) and (b) an emitting layer in the upper atmosphere, uniform as seen from the center of the earth but not uniform as seen from the earth's surface. The problem of coping with a non-uniform sky has not been solved (except for the special case of a single point source such as the sun) and, therefore, the use of the Ashburn tables introduces some errors, fortunately small, when applied to an actual sky in which both the astronomical (zodiacal light, Milky Way) and the airglow (dependence on azimuth) components are not uniform.

The principal difficulty in practice is that the Ashburn constants require multiplication by an average sky brightness as seen outside the scattering atmosphere. It is not possible to utilize for this purpose any particular region of the sky such as the zenith which is frequently strongly affected by the Milky Way. We have, therefore, made an estimate of the "average" sky brightness, J , for purposes of obtaining the scattering correction by an approximation technique. This is best shown by indicating analytically our data processing procedure. We define the following quantities:

z = zenith distance,

A = azimuth,

$m(z)$ = air mass from Haleakala,

τ_1 = extinction coefficient to refer a reading to
outside the atmosphere,

τ_2 = extinction coefficient to refer a reading to
outside the lower atmosphere but just inside
the ozone layer,

τ_3 = molecular (Rayleigh) coefficient,

J = average brightness of a uniform sky corresponding
to the actual non-uniform sky just inside the
ozone layer,

$Sc(z)$ = scattering factor from Ashburn's tables to be
multiplied into J ,

$V(z)$ = the van Rhijn function giving the increase with
zenith distance of an airglow layer as seen from
the surface of the earth,

$R(z,A)$ = the observed reading at z and A ,

$L(z)$ = the slant brightness in reading units of the
sky just inside the ozone layer.

The observed brightness in reading units can be defined as

$$R(z,A) = L(z)e^{-\tau_2 m(z)} + Sc(z) \cdot J. \quad (1)$$

Assuming the upper atmosphere component of J as 25% and the infinity component as 75%*, then

$$L(z) = .25 \cdot V(z) \cdot J + .75 \cdot J. \quad (2)$$

Substituting $L(z)$ from equation (2) into equation (1), we find

$$J = R(z,A)/[(.25 \cdot V(z) + .75)e^{-\tau_{2m}(z)} + S_c(z)]. \quad (3)$$

J was determined for each survey by computing it for each zenith distance and azimuth observed and taking the average of the 1800 (360 azimuth readings for each of 5 zenith distances) computations. Finally, we arrive at an expression for the brightness in absolute units [$S_{10}(\text{vis})$] outside the atmosphere by the formula

$$I(o/a) = [R(z,A) - S_c(z)J]e^{\tau_{1m}(z)} \cdot Q \quad (4)$$

where Q is the calibration constant to refer our galvanometer readings to $S_{10}(\text{vis})$ units of brightness. For a discussion of the $S_{10}(\text{vis})$

*The scattering correction is relatively insensitive to the assumed percentage of infinity and atmospheric light. As we have later determined (Table 4), it would have been better to have used a lower percentage for the airglow component. We did not repeat the calculations to correspond to the deduced percentages of airglow (Table 4) since the effect on the final result would have been small.

unit and of the methods we have used to evaluate Q , we refer to Roach and Smith⁽⁵⁾. Table 2 is a summary of the constants used in equations (3) and (4).

III. THE INTEGRATED STARLIGHT

As mentioned above, we avoided regions of the sky with galactic latitudes smaller than 30° *. In a recent study, Roach and Smith⁽⁵⁾ concluded that the integrated starlight for high galactic latitudes deduced from the Groningen 43⁽⁶⁾ star counts [see Roach and Megill⁽⁷⁾] represents the true integrated starlight when multiplied by 1.26. In the present study, we have taken 1.26 times the integrations from Groningen 43 for our estimations of the photometric effect of the integrated starlight. A point by point evaluation of the integrated starlight was made by a double interpolation between the values obtained from the tabular entries in Groningen 43.

The magnitude of the integrated starlight corrections is indicated in Table 3 in which the average values are given for selected galactic latitudes.

*The single exception is the ecliptic pole for which the galactic latitude is 28° .

IV. THE AIRGLOW CONTINUUM

The filter of our photometer was chosen so as to avoid any bright airglow emissions. Nevertheless, the presence of an airglow "continuum" in our observations is indicated by the systematic increase of the measured intensities toward the horizon. Such an increase has long been associated with the presence of an airglow component in the observations (the so-called van Rhijn effect). In a later study, we propose to go into the airglow problem in detail and here record in Table 4 the absolute airglow brightness used for each of the nights in the present analysis.

The airglow continuum was as much as 24% of the total light (J), but that this percentage does change significantly from night to night is indicated by the spread in the values listed in Table 4. Changes during a night and variations of brightness with azimuth were ignored in our treatment and errors due to ignoring these changes contribute slightly to the scatter in our final results. We refer to such errors as "subtractive" since they arise from uncertainties in subtracting out the non-zodiacal light components.

V. THE OBSERVATIONAL RESULTS

The numerical results of our study are assembled in Table 5 in the form of zodiacal light brightnesses over the observable domain

with 5° intervals in the parameters ecliptic latitude, β , and the differential ecliptic longitude, $\lambda - \lambda_0$.

In Fig. 1 the ensemble of data is plotted as isophotes in polar coordinates, β and $\lambda - \lambda_0$. The center of the plot is the ecliptic pole and the periphery is the ecliptic. In our analysis, we have averaged evening and morning results which correspond to the upper and lower parts of the plot which are thus mirror images of each other.

VI. DISCUSSION

The gross characteristic that stands out from an inspection of Fig. 1 is the contrast between the left and right halves of the plot. The right half represents intensities due to light originating from the dark or night side of the earth if one considers the problem in its diurnal context. It is probably preferable to consider it as a solar system problem and in this sense the right half of the plot is due to light from beyond the earth's orbit. The gegenschein shows as a small enhancement at $\lambda - \lambda_0 = 180$. There is a steady decline in brightness toward the ecliptic pole, but the distortion of the isophotes just on the sunward side of the pole gives an illusion that the center of the photometric minimum is not centered on the pole itself. On the left side of the plot, a dramatic increase of brightness is noted. The very bright zodiacal light [$> 1000 S_{10}(\text{vis})$] is brighter than most of our present observations and is shown without structure.

We show in Fig. 2 a plot of the zodiacal light brightness as a function of the ecliptic latitude for a differential ecliptic longitude, $\lambda - \lambda_0$, of 90° , a value chosen since it corresponds to a constant elongation, ϵ , of 90° over the whole plot*. The brightness goes steadily down from 250 $S_{10}(\text{vis})$ at the ecliptic to 110 $S_{10}(\text{vis})$ at the pole.

In Fig. 3 we show the brightness of the zodiacal light as a function of ϵ for two cases: (a) in the plane of the ecliptic where $\epsilon = \lambda - \lambda_0$, and (b) perpendicular to the plane of the ecliptic where $\epsilon = \beta$ for $\lambda - \lambda_0 = 0^\circ$ up to $\beta = 90^\circ$ and where $\epsilon = 180^\circ - \beta$ for $\lambda - \lambda_0 = 180^\circ$. The two curves come together at the gegenschein ($\epsilon = 180^\circ$) and would do so at the sun ($\epsilon = 0^\circ$) if we were able to carry our observations to that direction in space.

An interesting empirical quantity is the ratio, P , of the brightness of the zodiacal light at a given elongation in the ecliptic to that at the same elongation in a plane perpendicular to the ecliptic. For $\epsilon = 90^\circ$ we note that $P = \frac{250}{110} = 2.27$. We have attempted to make an approximate evaluation of P over the domain from the sun to the gegenschein based on a number of published sources plus the observations of this study. The last row (for $\lambda - \lambda_0 = 0^\circ$) in Table 5

*The elongation, ϵ , is conveniently derived from the expression: $\cos \epsilon = \cos (\lambda - \lambda_0) \cos \beta$.

contains a number of entries in parentheses* which represent graphical extrapolations down each column. These numbers are included in Table 6 in the column headed "Brightness, \perp ecliptic". The three entries in the "in ecliptic" column for 15° , 20° and 25° elongation are from Table III in Ingham⁽⁸⁾ with a factor of 1.20 found empirically necessary to put his observations into our scale**.

The ratio, P, must necessarily be unity at elongations of 0° (the sun) and 180° (the gegenschein). Any photometric concentration toward the ecliptic requires that the ratio be greater than one at intermediate elongations. An inspection of Fig. 4 indicates a maximum ratio of almost 5 at an elongation of 35° . We suggest that a refinement of Fig. 4 might be an interesting observational goal.

In the region between $\epsilon = 50^\circ$ and 90° in the plot of Fig. 4, a departure of P from the smooth curve (as dashed by us) is noted.

*The quantities within parentheses in the first two columns also represent graphical extrapolations, but in this case, the reason for the extrapolation was to attempt to allow for the slow time response of our recording galvanometer.

**Example: At $\epsilon = 35^\circ$, Ingham records a brightness of 1340 compared to our value of 1595.

When this came to our attention in the early examination of the data, we made a concentrated study of the region. Inspection of Fig. 1 demonstrates that the photometric irregularity seems to persist away from the $\lambda - \lambda_{\odot} = 0^{\circ}$ domain as evidenced by the 200 $S_{10}(\text{vis})$ islands near $\beta = 55^{\circ}$ and $\lambda - \lambda_{\odot} = 45^{\circ}$ (corresponding to $\epsilon = 66^{\circ}$). We cannot detect any such perturbation extending down to the ecliptic in the $\epsilon = 65^{\circ}$ ($\lambda - \lambda_{\odot} = 65^{\circ}$ also) region*. It should be remarked that the region of enhancement was included in our records over almost a 4-month period from August 14/15 to November 6/7, 1961, a period during which the position of the Milky Way in the sky permitted a definitive test.

In order to indicate the evidence for the excess which led to the $S_{10}(\text{vis}) = 200$ islands in Fig. 1, we show in Fig. 5 plots of the brightness versus differential elongation for a family of values of β from 25° to 80° . The region of excess is seen as a progression of maxima especially in the curves for $\beta = 45^{\circ}$, 50° and 55° . In Fig. 6 we have isolated the excess in the plane perpendicular to the ecliptic based on the departure of the distorted region (Fig. 4) from the smooth curve (dashed) indicating a brightness of some 50 $S_{10}(\text{vis})$ units.

*In a detailed plot of the zodiacal light brightness in the ecliptic by Weinberg⁽²⁾, there is a hint of a slight enhancement in the $\epsilon = 65^{\circ}$ region.

We assume the privilege of the observer to be the first to speculate about the physical significance of his own observations and suggest that the excess may be due to a concentration of scattering material some 50° to 90° from the sun in the general region away from the ecliptic. If this be the explanation then a localized (with respect to the earth) concentration seems to us more reasonable than one extending over some 120° of ecliptic longitude over the four months that the excess was observed.

VII. CONCLUSIONS

From systematic photometric observations of the night sky at the Haleakala Observatory, we have isolated the zodiacal light component and recorded it in terms of ecliptic coordinates. We find a photometric ecliptic enhancement of 4.88 at its maximum for an elongation of 35° and of 2.27 at an elongation of 90° . We find evidence for a photometric perturbation some 70° from the sun in regions well away from the ecliptic.

VIII. ACKNOWLEDGMENTS

It is a pleasure to acknowledge the help we have received from several colleagues in the prosecution of this study. We are indebted to Mr. H. M. Mann and to Mr. H. Tanabe for obtaining the original photometric records; to Dr. Robert Sparks for assistance

in several aspects of the use of the University of Hawaii computing facilities; and to Mr. George Sugar of the National Bureau of Standards for his contribution to the program through his design of the equipment for digitizing our records. We particularly express our thanks to Professor Walter Steiger for many courtesies extended to us during the 1963-64 period, during which we initiated this report as guests of the Hawaii Institute of Geophysics. One of us (FER) gratefully acknowledges the debt he owes to the East-West Center of the University of Hawaii as a recipient of a Senior Research Scholarship for the 1963-64 period. A part of the expense of the investigations was covered by NASA Grant R 18.

REFERENCES

1. D. Barbier, F. E. Roach, and W. R. Steiger, J. Research NBS 66D, 145 (1962).
2. J. L. Weinberg, PhD. dissertation, University of Colorado (1963).
3. C. M. Purdy, L. R. Megill, and F. E. Roach, J. Research NBS 65C, 213 (1961).
4. E. V. Ashburn, J. Atmospheric Terrest. Phys. 5, 83 (1954).
5. F. E. Roach and L. L. Smith, NBS Tech. Note 214 (1964).
6. P. J. van Rhijn, Groningen Publication No. 43 (1925).
7. F. E. Roach and L. R. Megill, Astrophys. J. 133, 228 (1961).
8. M. F. Ingham, Monthly Notices Roy. Astron. Soc. 122, 157 (1961).
9. F. E. Roach and A. B. Meinel, Astrophys. J. 122, 530 (1955).
10. C. W. Allen, Astrophys. Quant. p. 116 (1955).
11. R. Michard, A. Dollfuss, J. C. Pecker, M. Laffineur, and Mme. M. d'Azambuja, Ann. d'Astrophys. 17, 4 (1954).

Table 1

The Six Nights Included in this Study

Night	Period of Observations				Number of Sky Surveys
	Beginning		End		
	H.S.T. (hrs.:mins.)	Sid Time (degrees)	H.S.T. (hrs.:mins.)	Sid Time (degrees)	
1961					
Aug. 14/15	21:00	272	04:55	31	96
Sept. 11/12	19:40	280	04:55	59	112
Nov. 6/7	22:55	23	05:30	122	79
1962					
Feb. 3/4	19:45	63	05:30	210	117
March 31/ Apr 1	19:50	120	04:10	245	99
June 27/28	20:30	217	03:20	319	82
					585 (total)

Table 2

Constants Used in the Reduction of the Data

z	m(z)	τ			$\tau_m(z)$			τ_e		Sc(z)	V(z) h=100km
		$\tau_1^{(u)}$	$\tau_2^{(u)}$	$\tau_3^{(u)}$	$\tau_1^m(z)$	$\tau_2^m(z)$	$\tau_3^m(z)$	for $\tau_1^m(z)$	for $\tau_2^m(z)$		
0	0.684	0.142	0.121	0.112	0.097	0.083	0.077	1.102	1.087	0.047	1.000
40	0.889	"	"	"	0.126	0.108	-	1.135	1.114	0.061	1.292
60	1.363	"	"	"	0.194	0.166	-	1.214	1.181	0.093	1.914
70	1.984	"	"	"	0.282	0.240	-	1.326	1.271	0.131	2.635
75	2.613	"	"	"	0.371	0.316	-	1.449	1.372	0.163	3.234
80	3.830	"	"	"	0.544	0.463	-	1.723	1.589	0.238	4.085

(1) From Weinberg⁽²⁾.(2) $\tau_2 = \tau_1 - .021$ (ozone absorption, Roach and Meinel⁽⁹⁾).(3) From Allen⁽¹⁰⁾.

TABLE 3

Mean Integrated Starlight

Galactic Latitude	Mean Integrated Starlight (from Groningen 43) in $S_{10}(\text{vis})$ units	Mean Integrated Starlight used (1.26 X GR 43)
80	31.1	39.2
70	32.5	41.0
60	35.5	44.7
50	41.3	52.0
40	51.5	64.9
30	68.7	86.6

Table 4
The Airglow Continuum

Date	Airglow Continuum ($S_{10}(\text{vis})$)						Mean J	Percent Airglow zenith Mean J
	z = 0	40	60	70	75	80		
1961								
Aug 14/15	60	75	115	160	195	255	285	21
Sep 11/12	60	75	115	160	195	260	305	20
Nov 6/7	60	100	155	215	265	355	330	24
1962								
Feb 3/4	20	25	40	55	65	85	245	8
Mar 31/Apr 1	45	60	95	130	160	210	300	17
Jun 27/28	50	65	100	140	170	225	305	16

Table 5

Brightness of the Zodiacal Light in Ecliptic Coordinates

$\lambda - \lambda_0$	0	5	10	15	20	25	30	35	40	45	50	55	60	65	70	75	80	85	90			
180	205	195	185	175	165	155	150	140	125	130	125	125	125	125	115	115	115					
175	195	190	175	165	160	150	150	135	125	130	125	125	125	125	115	115	115					
170	185	175	170	160	155	150	145	135	125	130	120	125	125	125	115	115	115					
165	175	170	165	160	150	145	145	135	125	130	120	125	125	125	115	115	115					
160	175	170	160	155	145	145	145	135	125	130	125	120	125	125	115	115	115					
155	170	165	160	155	150	145	145	135	125	130	125	125	125	125	115	115	115					
150	170	165	160	155	150	150	145	140	125	130	125	125	125	125	115	115	110					
145	175	170	165	155	155	155	145	140	125	135	130	125	125	125	115	115	110					
140	175	170	165	160	155	155	145	145	130	135	130	120	125	125	115	115	115					
135	175	170	170	160	160	155	145	145	135	135	135	120	125	125	115	115	115					
130	175	175	170	165	160	155	145	145	135	135	135	125	125	125	115	115	115					
125	180	175	175	165	165	160	145	145	135	135	135	125	125	125	115	115	115					
120	185	180	180	170	165	160	145	150	135	135	135	125	125	125	120	115	115					
115	190	185	180	175	170	165	150	150	135	135	135	125	125	120	120	115	115					
110	200	190	185	175	170	165	150	150	140	135	135	125	125	120	120	115	115					
105	210	200	190	180	175	170	150	150	145	135	135	130	125	120	120	115	115					
100	220	205	195	185	175	170	155	150	145	135	135	130	125	120	120	115	115					
95	235	215	205	190	180	170	155	155	150	135	135	130	125	125	120	120	120					
90	250	235	215	200	185	175	155	160	150	135	135	130	125	125	125	125	125					
85	265	255	235	215	195	180	155	165	155	135	140	130	125	125	125	125	130					
80	290	275	255	230	210	190	165	170	155	135	140	130	125	125	125	125	130	110				
75	320	300	285	245	225	200	185	175	160	135	145	130	125	130	125	130	130	110				
70	(370)	335	310	265	240	210	205	185	175	145	145	130	135	135	130	135	130	115				
65	(425)	370	345	285	255	225	205	205	200	170	150	140	140	140	130	135	130	115				
60	(500)	425	380	305	270	240	215	205	205	195	165	145	145	145	135	135	130	115				
55	(600)	505	430	330	290	255	225	205	205	200	180	160	155	150	135	135	135	120				
50	(745)	610	485	370	315	285	230	205	205	195	205	170	160	150	140	140	135	120				
45	(945)	735	555	425	345	315	240	215	210	190	205	190	170	155	140	140	135	120				
40	(1185)	870	655	505	390	360	250	220	215	190	195	205	170	160	140	140	135	125				
35	(1595)	(1145)	845	690	450	410	270	225	215	190	185	200	175	165	145	145	140	125				
30	(2350)		905	545	465	520	300	230	220	195	180	195	185	170	145	150	145	125				
25								245	225	200	180	190	190	175	150	150	145	130				
20								230	230	205	180	185	190	180	150	150	145	135				
15								235	235	205	180	180	185	185	155	155	150					
10									210	210	180	175	185	185	155	155	150					
5												175		185	155	160						
0												(6150)	(1820)	(995)	(525)	(330)	(250)	(215)	(180)	(185)	(150)	(135)

Table 6

Brightness of the Zodiacal Light in the Plane of the
Ecliptic and in a Plane Perpendicular to the Ecliptic

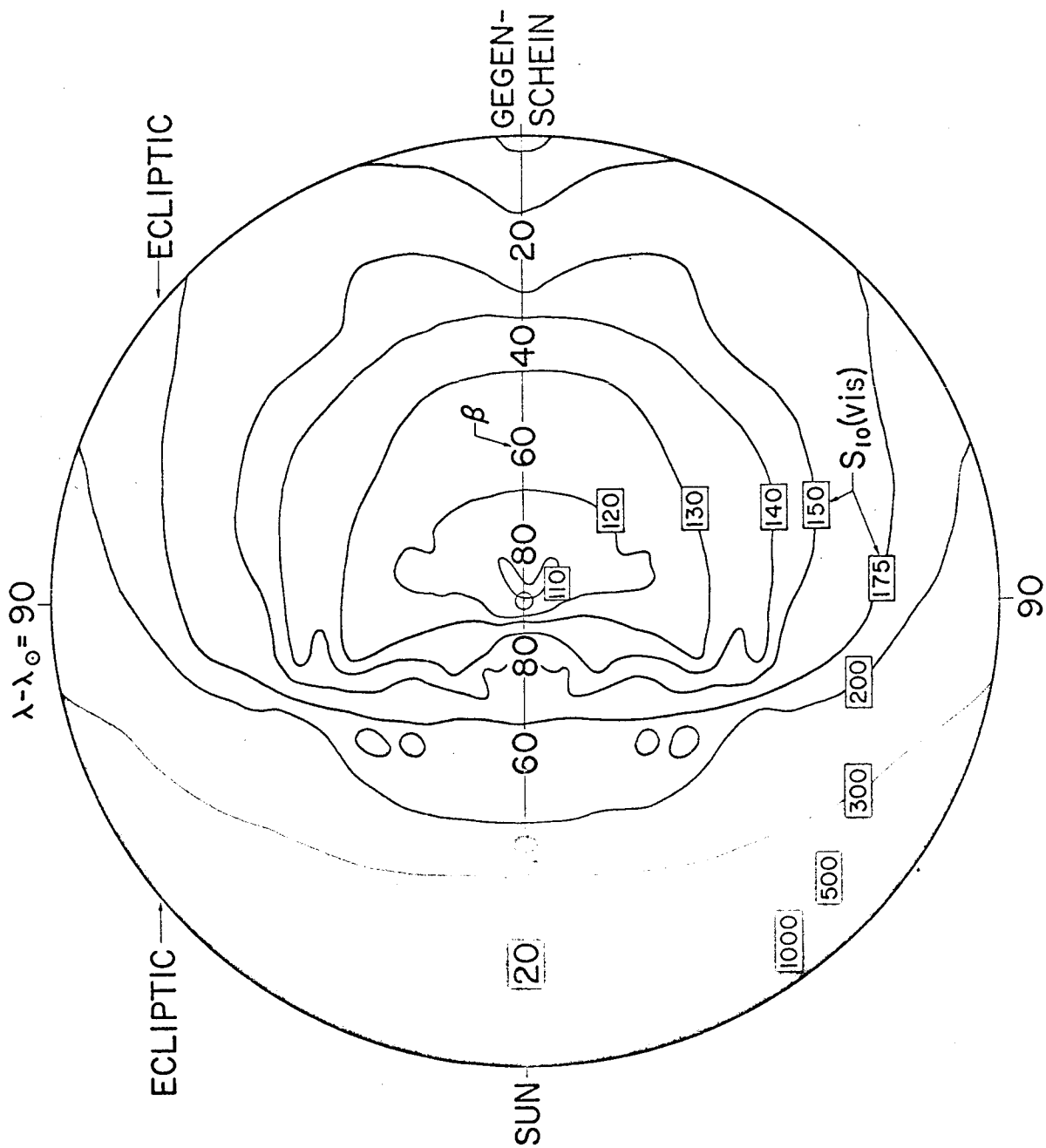
Elongation, ϵ	Brightness, $S_{10}(\text{vis})$		Ratio, P	Elongation, ϵ	Brightness, $S_{10}(\text{vis})$		Ratio, P
	In ecliptic	\perp ecliptic			In ecliptic	\perp ecliptic	
2°40'	966,400*	634,300*	1.52	95	235	110	2.14
5°20'	240,200*	137,600*	1.75	100	220	115	1.91
15	13,800**	6150	2.24	105	210	115	1.83
20	6200**	1820	3.41	110	200	115	1.74
25	3640**	995	3.66	115	190	125	1.52
30	2330	525	4.44	120	185	125	1.48
35	1595	330	4.88	125	180	125	1.44
40	1185	250	4.74	130	175	125	1.40
45	945	215	4.40	135	175	130	1.35
50	745	180	4.14	140	175	125	1.40
55	600	175	3.43	145	175	140	1.25
60	500	185	2.70	150	170	150	1.13
65	425	185	2.30	155	170	155	1.10
70	370	155	2.39	160	175	165	1.06
75	320	160	2.00	165	175	175	1.00
80	290	150	1.93	170	185	185	1.00
85	265	135	1.96	175	195	195	1.00
90	250	110	2.27	180	205	205	1.00

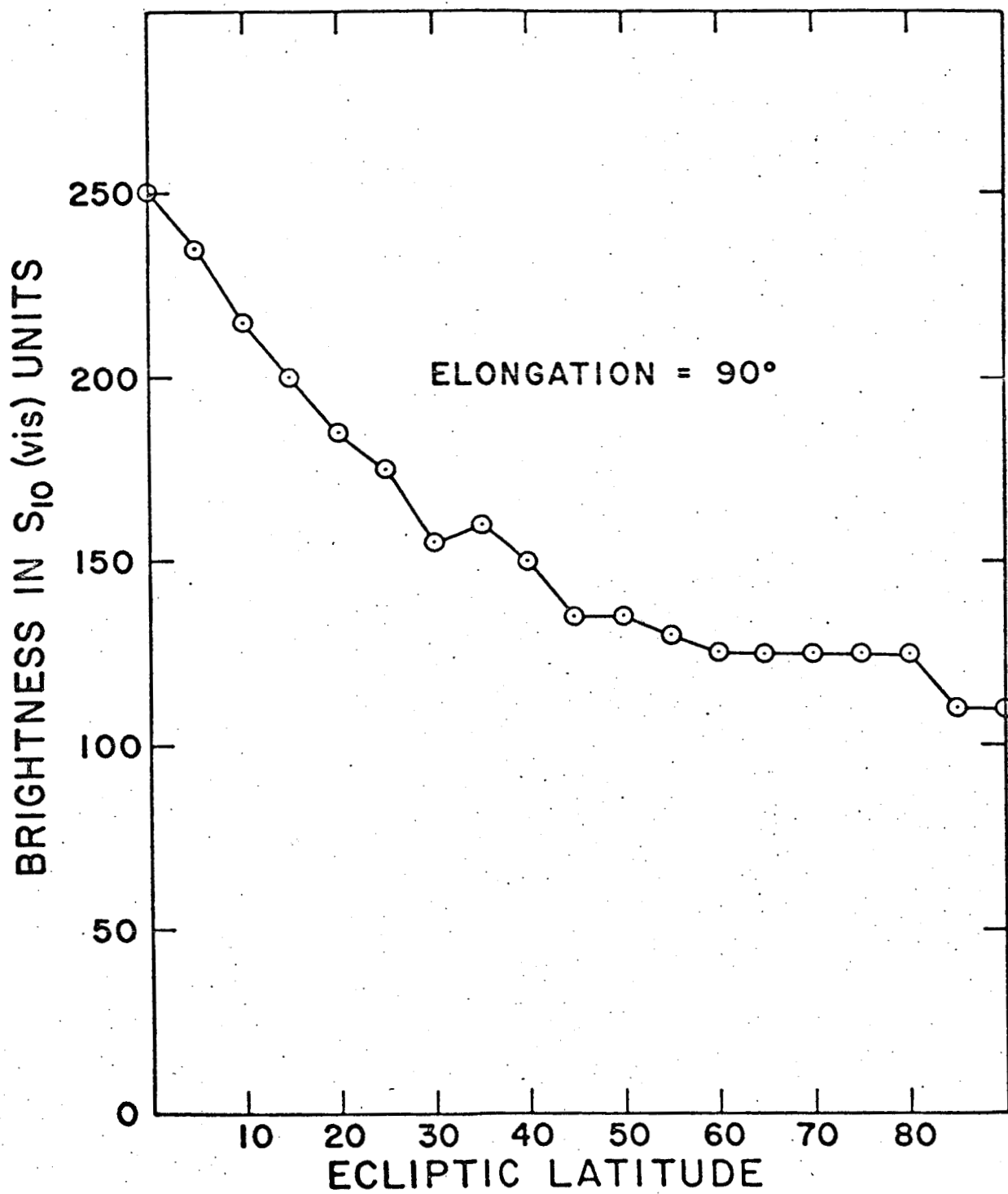
* From Michard et al. (11).

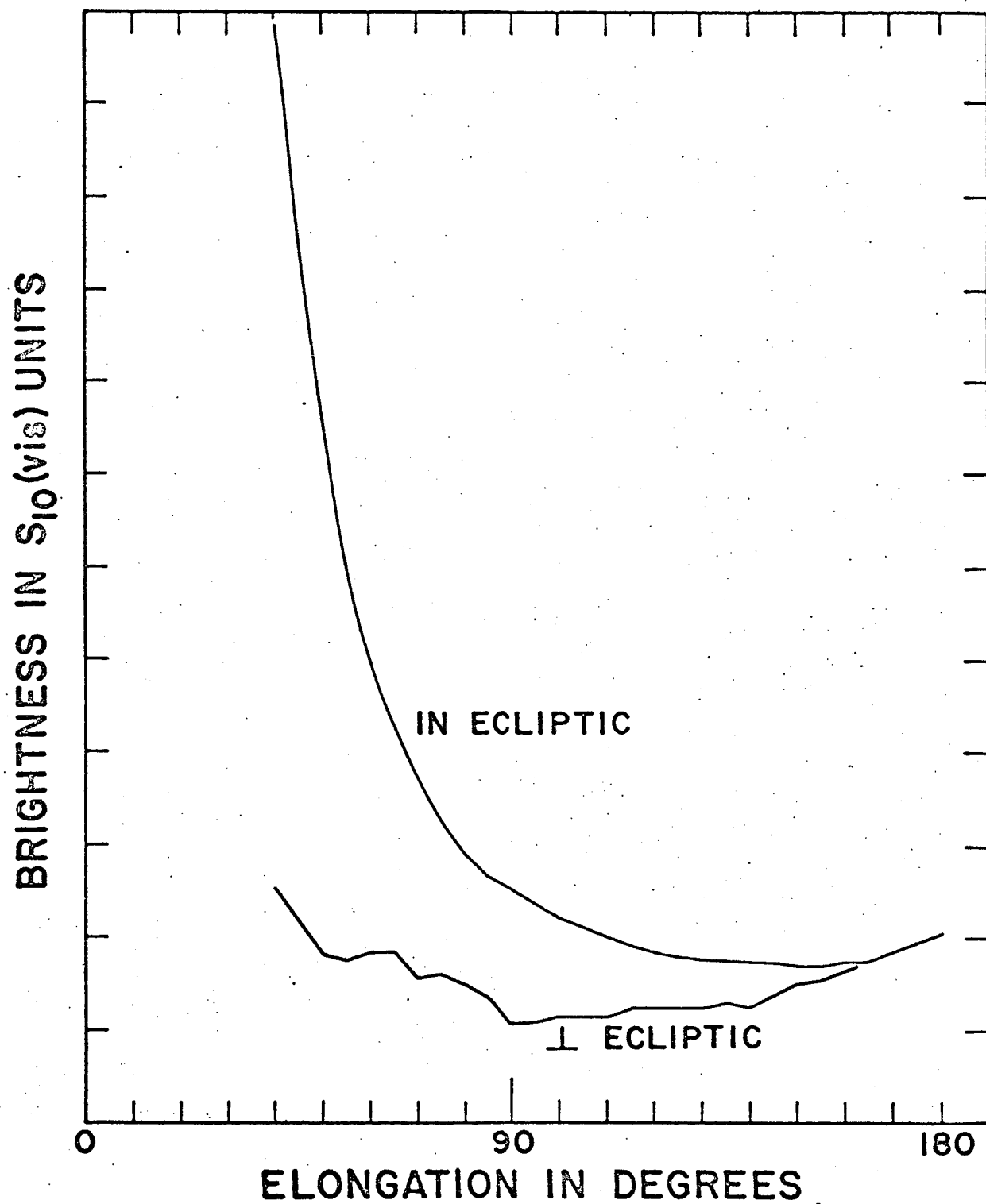
** From Ingham (8) (Table III) multiplied by 1.20.

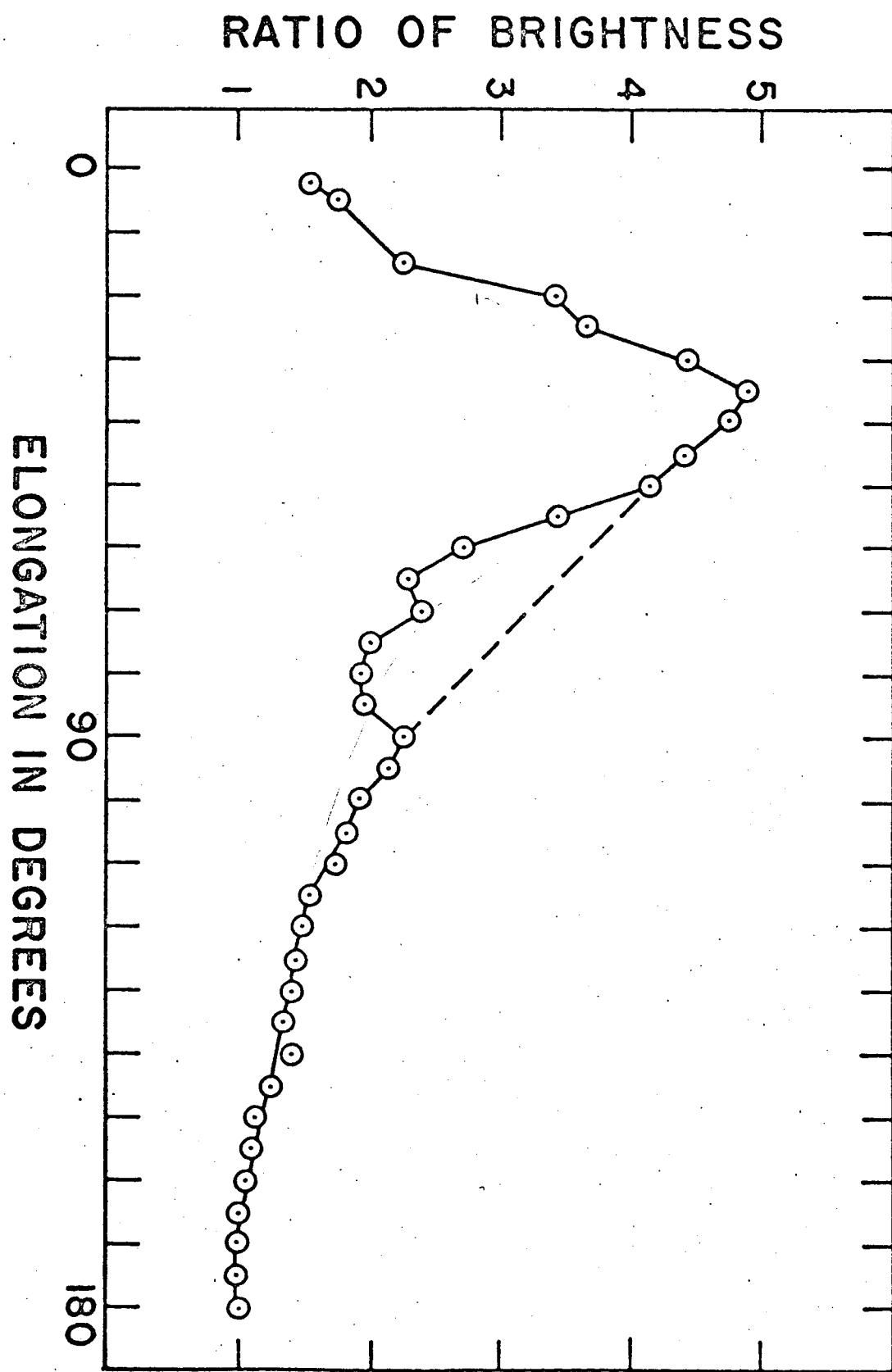
LEGEND FOR FIGURES

- Fig. 1. Isophotal map of the zodiacal light in polar coordinates. The circumference represents the plane of the ecliptic with values of differential longitude, $\lambda - \lambda_0$, increasing from 0° to 90° to 180° (the gegenschein). The ecliptic latitude, β , increases from 0° at the ecliptic to 90° in the center of the circle.
- Fig. 2 Brightness of the zodiacal light as a function of ecliptic latitude for an elongation of 90° .
- Fig. 3 Brightness of the zodiacal light as a function of the elongation for two planes: above in the ecliptic, below at right angles to the ecliptic. The gegenschein is the slight rise at $\epsilon = 180^\circ$.
- Fig. 4 Ratio of brightness of the zodiacal light in the ecliptic to that in a plane at right angles to the ecliptic as a function of elongation from the entries in Table 7.
- Fig. 5 Brightness of the zodiacal^{light} as a function of differential longitude for ecliptic latitudes ranging from 25° to 80° . The successive curves are displaced from each other by $50 S_{10}(\text{vis})$ units.
- Fig. 6 Brightness of the excess zodiacal light in a plane perpendicular to the ecliptic as a function of elongation. The excess is thought to be due to a terrestrial component (see text).









BRIGHTNESS IN $S_{10}(\text{vis})$ UNITS

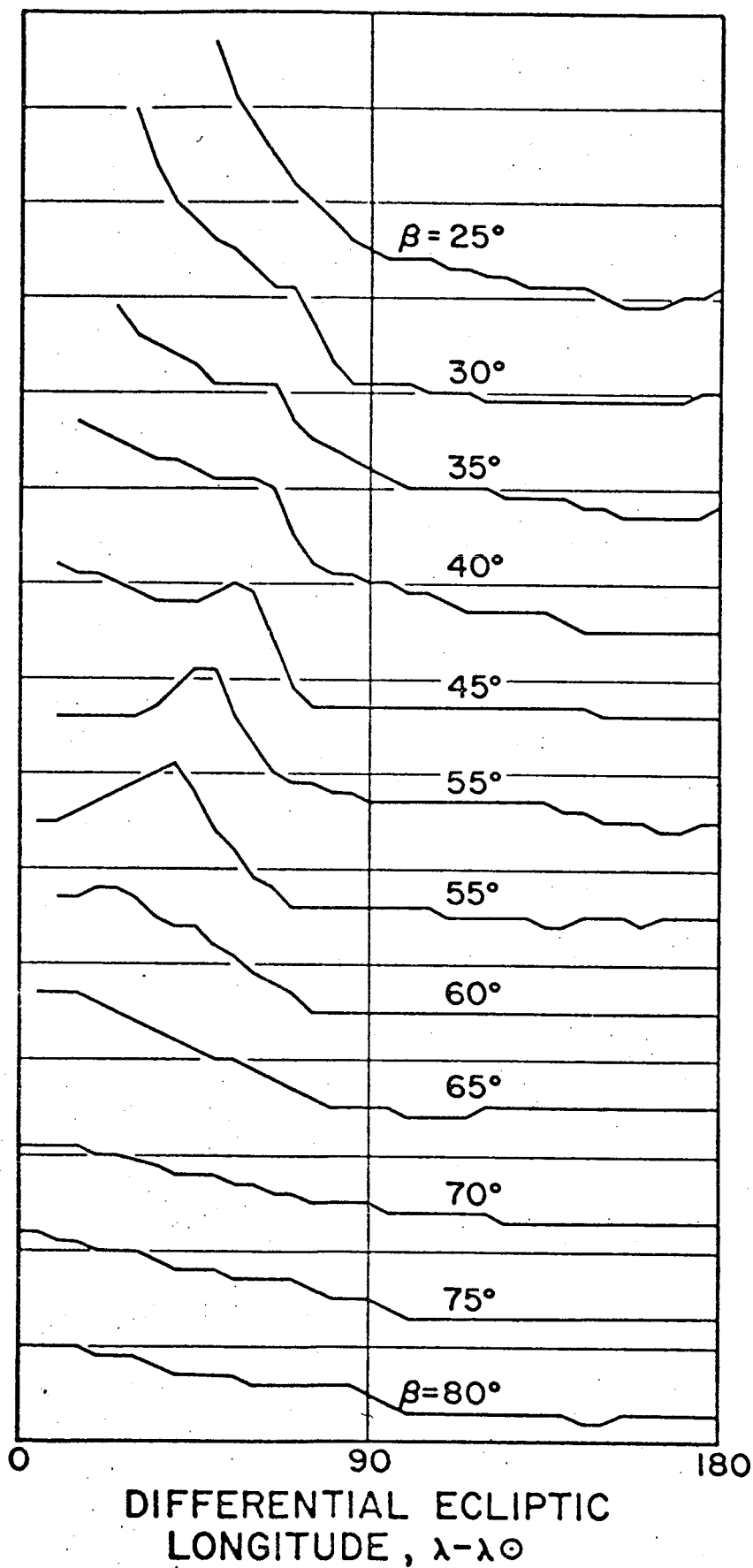


FIGURE 6

